

DESY 82-029
May 1982



HIGHER ORDER QCD CORRECTIONS FOR e^+e^- ANNIHILATION

JET CROSS SECTIONS - A REEVALUATION

by

G. Kramer

II. Institut für Theoretische Physik der Universität Hamburg

NOTKESTRASSE 85 · 2 HAMBURG 52

DESY behält sich alle Rechte für den Fall der Schutzrechtserteilung und für die wirtschaftliche Verwertung der in diesem Bericht enthaltenen Informationen vor.

DESY reserves all rights for commercial use of information included in this report, especially in case of apply for or grant of patents.

**To be sure that your preprints are promptly included in the
HIGH ENERGY PHYSICS INDEX ,
send them to the following address (if possible by air mail) :**

**DESY
Bibliothek
Notkestrasse 85
2 Hamburg 52
Germany**

DESY 82-029
May 1982

1. Introduction

Since 1980 several groups have calculated higher order QCD corrections (up to $O(\alpha_s^2)$) to jet distributions which describe details of e^+e^- annihilation into hadrons [1,2]. Such calculations of higher order corrections are important for several reasons. First, only if the higher order contributions come out sufficiently small, we can consider the apparent consistency of theory and experiment in lowest order QCD, which has been established in many areas in the last five years, a meaningful test of the theory. Second, the non-abelian gauge structure shows up only in contributions of order α_s^2 and higher. Third, it is well known, that a meaningful determination of the coupling constant α_s or the scale parameter Λ is only possible, if at least the $O(\alpha_s^2)$ corrections are known, since the prescription dependence of α_s or Λ remains undefined in lowest order [3].

The unique quantity, which can be measured and for which $O(\alpha_s^2)$ corrections have been calculated, is the famous R value, i.e. the ratio of the total e^+e^- annihilation cross section σ_{tot} divided by $\sigma(e^+e^- \rightarrow \mu^+\mu^-)$, which is [4]

$$R = 3 \sum_{f=1}^{N_f} \alpha_f^2 \left(1 + \frac{\alpha_s}{\pi} + (1.986 - 0.115 N_f) \left(\frac{\alpha_s}{\pi} \right)^2 \dots \right) \quad (1.1)$$

In (1.1) the coupling constant α_s is defined in the \overline{MS} scheme. The most recent determination of α_s , using experimental data for R comes from the TASSO group of PETRA [5]. They find, including the contributions from weak interactions, for α_s the value

$$\alpha_s = 0.24 \pm 0.05 \pm 0.13 \quad (1.2)$$

This value of α_s from R measurements can hardly be improved in the future because the systematic error which is given by ± 0.13 in (1.2) cannot be lowered substantially.

Higher Order QCD Corrections for e^+e^- Annihilation

Jet Cross Sections - A Reevaluation. ++

by

G. Kramer

II. Institut für Theoretische Physik⁺ der Universität Hamburg

⁺ supported by Bundesministerium für Forschung und Technologie, Bonn

⁺⁺ Talk presented at the 13th Spring Symposium on High Energy Physics, Haidemühle, Bad Schandau.

The higher order corrections to R are rather small, of the order of $(\frac{\alpha_s}{\pi})^2$, which is equal to 0.29% as compared to 1 for $\alpha_s = 0.17$. This would indicate that the corrections to differential distributions of jet cross sections should be of this order of magnitude also. Actually this is not necessarily true. For example, it is well known, that the 4-jet cross section becomes large if infrared sensitive regions of phase space are included in $\sigma(4\text{-jet})$ [6]. Such a large 4-jet cross section is compensated by equally large negative 3-jet and 2-jet contributions so that the $O(\alpha_s^2)$ contribution to σ_{tot} comes out as given in (1.1). Whether higher order corrections to jet cross sections of a specified number of jets is large or small depends very much on how much of the infrared sensitive region of phase space is included.

Since there is little hope to determine α_s from measurements of R the best quantity to obtain α_s is the 3-jet cross section as measured in PEPPA and PEP experiments. Fitting the $O(\alpha_s)$ thrust or sphericity distributions to the measured cross sections all groups obtained values for α_s between 0.15 and 0.17 for center of mass energies $q^2 = 30$ GeV. But concerning the $O(\alpha_s)$ corrections, for example to the thrust distribution $\frac{1}{\sigma} \frac{d\sigma}{d\tau}$, two apparently differing results were obtained. In 1 the sum of the 3-jet and 4-jet thrust distribution was calculated up to $O(\alpha_s)$ with the result that $\frac{1}{\sigma} \frac{d\sigma}{d\tau}$ increased roughly by a factor of 2 as compared to $\frac{d\sigma}{d\tau}$ in $O(\alpha_s)$ if $\alpha_s = 0.16$. Part of this increase is certainly due to the 4-jet contribution which was not present in the $O(\alpha_s)$ thrust distribution. In another calculation [2] the authors started with infrared divergent 3- and 4-parton cross sections and introduced physically distinguishable jets.

$$d\sigma_{\text{jet}} = d\sigma_{3\text{-jet}} + d\sigma_{4\text{-jet}} \quad (1.3)$$

Here the 3-jet cross section consisted of all 3-parton terms, i.e. the $O(\alpha_s)$ terms and the $O(\alpha_s^2)$ virtual corrections, and those parts of the 4-parton cross section in which two of the four partons were irresolvable. Two partons were said to be irresolvable if

either parton has energy less than $\frac{q^2}{2}$ or the angle between the two partons is less than δ . Therefore $d\sigma_{3\text{-jet}}(\epsilon, \delta)$ is the cross section for events with fraction $(1-\epsilon/2)$ of the total energy distributed within three separated cones of opening angle δ (see Fig. 1) and $d\sigma_{4\text{-jet}}(\epsilon, \delta)$ is what remains from the 4-parton contribution, this is the region where the fourth parton is outside the kinematic region given in Fig. 1. Examples for resolution equipped 3-jet cross section are shown in Fig. 2 for $(\epsilon, \delta) = (0.2, 45^\circ)$ and $(\epsilon, \delta) = (0.1, 30^\circ)$ and $\alpha_s = 0.17$. We see that the $O(\alpha_s^2)$ corrected cross section $\frac{d\sigma}{d\Omega}^{\text{cor}}$, where Ω_{max} is the 3-particle thrust, is smaller than the lowest order cross section. In order to have reasonable small corrections ϵ and δ must be chosen fairly large around $(\epsilon, \delta) = (0.2, 45^\circ)$. Of course, a comparison with experimental cross sections is possible if similar resolution equipped cross sections are defined which is possible with the help of well known cluster analysis [7]. Of course, the curves in Fig. 2 should not be compared to the results of ref. 7. For this purpose we must at least add the thrust distribution originating from $d\sigma_{4\text{-jet}}(\epsilon, \delta)$. This is shown in Fig. 3 (model I, [2]) together with $\frac{d\sigma}{d\tau}$ as obtained by Ellis et al. (model II, [1]) [8]. The results of all the other groups in ref. 1 agree with model II. In this figure the situation concerning the apparently differing results for $\frac{d\sigma}{d\tau}$ is summarized. We see that in model I the higher order corrections produce roughly a 40% correction as compared to the $O(\alpha_s)$ curve whereas in model II the correction is roughly 80%. It is clear that in order to fit the same experimental data with model II as with model I a much smaller coupling α_s would be needed which automatically would lead to a much smaller A value. At the Bonn conference the difference between the two curves was attributed to the fact that two different definitions for "thrust" were used in the two approaches [9]. Where as this may explain the differing results it does not clarify which is the correct approach for describing experimental data and for determining α_s and A . It is the purpose of this paper to shed further light on this problem. For this we have undertaken a completely new and independent evaluation of the appropriate jet cross

sections in which instead with our original ϵ and δ we use an invariant mass constraint for defining whether two partons are irresolvable or not. With this two partons i and j are said to be irresolvable if the invariant mass squared $(p_i + p_j)^2 = 2p_i p_j$ is less than yq^2 . This has the advantage that the criterium depends only on one parameter y which makes it easier to study how jet cross sections depend on y . Furthermore using invariant mass constraint brings us near to approaches used by the authors in [1], in which the four parton phase space was expressed by invariants $s_{ij} = (p_i + p_j)^2$ instead to momenta and angles as used in our original work [2].

In the next section we shall give the formulas for 3-jet distributions using the invariant mass constraint. We shall compare these formulas with a recent (preliminary) cluster analysis done by E.Elsen of the JADE group at PETRA [10]. This will yield a new value for α_s which can be compared with earlier determinations. In this section we shall discuss also the correct range of y values to be used in such an analysis.

In section 3 we study the sum of 3- and 4-jet cross sections as a function of y and discuss its relation to the results obtained by the authors in [1]. This will clarify, I hope, the relation of the two approaches [1] and [2].

In the last section we shall make some concluding remarks.

2. 3-Jet Cross Section with y Cut.

Before representing the results for the 3-jet cross section up to order α_s^2 we describe our method for the simpler case in $O(\alpha_s)$.

In lowest order of α_s we have two types of diagrams. First we have the virtual correction to the 2-parton term which contributes to the 2-jet cross section and is shown in Fig. 4. It produces an infrared divergent contribution proportional to α_s . This has to be combined with the bremsstrahlung contribution coming from the last

two diagrams in Fig. 4. Averaged over angles with respect to the beam direction this cross section has the familiar form:

$$\frac{1}{\sigma_0} \frac{d\sigma}{dy_13 dy_23} = \frac{\alpha_s}{2\pi} C_F T^V(y_{13}, y_{23}) \quad (2.1)$$

$$\text{where } T^V(y_{13}, y_{23}) = \frac{y_{13}}{y_{23}} + \frac{y_{23}}{y_{13}} + \frac{2 y_{12}}{y_{13} y_{23}} \quad (2.2)$$

Here $Y_{ij} = s_{ij}/q^2 = 2p_i p_j/q^2$ and p_1, p_2 and p_3 are the momenta of quark, antiquark and gluon respectively. $Y_{13} + Y_{23} + Y_{12} = 1$ so that T depends only on the two normalized invariants Y_{13} and Y_{23} . The phase space for Y_{13} and Y_{23} is shown in Fig. 5. T diverges for Y_{13} and/or $Y_{23} \rightarrow 0$. These singular regions of phase space up to some boundary parametrized by y have to be integrated over and added to the $O(\alpha_s)$ virtual 2-parton term. The sum yields the total 2-jet cross section. It includes those terms of the 3-parton final state where two of the three partons are irresolvable, which is given by the region

$$0 \leq Y_{13}, Y_{23} \leq y$$

shown in Fig. 5. The region $0 \leq Y_{12} \leq y$ is non-singular and contributes only terms $O(y)$, which will be neglected here. Of course, y should be chosen such that $y \ll 1$ otherwise the 2-jet cross section exhausts almost all $O(\alpha_s)$ contributions. But in principle y is arbitrary in the interval $0 < y \leq \frac{1}{2}$. The integration over the y -strip yields infrared and collinear singular terms, evaluated for example in n -dimensional regularization, which cancel the identical singular terms from the virtual diagram in Fig. 4. The result for the sum of the two terms is the 2-jet cross section

$$\sigma_{2\text{-jet}}(y) = \sigma_0 \left(1 + \frac{\alpha_s}{2\pi} C_F \left[-2 \ln^2 y - 3 \ln y - 1 + \frac{\pi^2}{3} + 4 \ln y \right] \right) \quad (2.3)$$

(2.3) includes also the lowest order contribution $\sigma_0 = \frac{4\pi\alpha_s^2}{3q^2} N_c \sum_{f=1}^{N_f} Q_f^2$

where $N_c = 3$, N_f is the number of flavours and $C_F = \frac{4}{3}$. In (2.3) we neglected terms $O(y)$ except the term $\sim y \ln y$. Therefore (2.3) can be used only for small enough y , so that terms $\sim y$, $\sim y^2 \ln y$ etc. are negligible. If we integrate (2.1) over the outer triangle in Fig. 5 we obtain the integrated 3-jet cross section which is

$$\sigma_{3\text{-jet}}^{\text{red}}(y) = \sigma_0 \frac{\alpha_s}{2\pi} C_F \left[2 \ln^2 y + 3 \ln y + \frac{5}{2} - \frac{\pi^2}{3} - 4 y \ln y \right] \quad (2.4)$$

Of course, the sum of $\sigma_{2\text{-jet}}$ and $\sigma_{3\text{-jet}}$ is independent of y and is

$$\sigma_{2\text{-jet}}^{\text{red}}(y) + \sigma_{3\text{-jet}}^{\text{red}}(y) = \sigma_0 \frac{\alpha_s}{2\pi} C_F \frac{2}{3} \quad (2.5)$$

Formula (2.3) replaces the well-known Sterman-Weinberg 2-jet formula with ϵ, δ -cuts [11]. Let us define the reduced 2-jet and 3-jet cross section by

$$\frac{\sigma_{2\text{-jet}}^{\text{red}}(y)}{\sigma_0} - 1 = \frac{\alpha_s}{\pi} \sigma_{2\text{-jet}}^{\text{red}}(y) \quad (2.6)$$

$$\frac{\sigma_{3\text{-jet}}^{\text{red}}(y)}{\sigma_0} = \frac{\alpha_s}{\pi} \sigma_{3\text{-jet}}^{\text{red}}(y) \quad (2.7)$$

Then $\sigma_{2\text{-jet}}^{\text{red}}(y)$ is just the $O(\alpha_s)$ contribution to $\sigma_{2\text{-jet}}$ in units of σ_0 without the factor $\frac{\alpha_s}{\pi}$ and similarly $\sigma_{3\text{-jet}}^{\text{red}}(y)$ is the 3-jet cross section in units of σ_0 without the factor $\frac{\alpha_s}{\pi}$. These two cross sections are plotted as a function of $\ln y^{-1}$ in Fig. 6. $\sigma_{3\text{-jet}}^{\text{red}}(y)$ is positive and increases with $\ln y^{-1}$ and $\sigma_{2\text{-jet}}^{\text{red}}(y)$ is negative of almost equal magnitude. Of course, the sum of both is equal to

$$\sigma_{3\text{-jet}}^{\text{red}}(y) + \sigma_{2\text{-jet}}^{\text{red}}(y) = 1 \quad (2.8)$$

which is near the axis in Fig. 6. This is just the $O(\alpha_s)$ contribution to σ_{tot} without the factor $\frac{\alpha_s}{\pi}$. Fig. 6 teaches us that y values, which are smaller than 0.01 do not make sense. For $y^{-1} = 100$ we have $\sigma_{3\text{-jet}}^{\text{red}} \simeq -\sigma_{2\text{-jet}}^{\text{red}} \simeq 20$ which makes $\sigma_{2\text{-jet}}^{\text{red}}(y=0.01) \simeq 0$ and $\sigma_{3\text{-jet}}^{\text{red}}(y=0.01) \simeq \sigma_{\text{tot}}$ for a realistic $\frac{\alpha_s}{\pi} = 0.05$. This means that for $y < 0.01$ perturbation theory breaks down and $\sigma_{2\text{-jet}}$ becomes negative and $\sigma_{3\text{-jet}}$ larger than σ_{tot} . On the other hand too large values for y should be avoided also, because the approximation of neglecting terms $\sim y$ and $\sim y^2 \ln y$ breaks down. This is certainly the case for $y > 0.1$, where terms of order y produce a correction of roughly 5%. To be on the safe side, we consider y 's in the interval $0.05 \lesssim y \lesssim 0.02$ a reasonable range. So only a rather small window for invariant mass cut-off values is possible if one requires that finite order perturbation theory should make sense. These considerations apply equally well to higher orders. The reason is, that cross sections for the production of a definite number of jets are calculated in perturbation theory as a series in an expansion parameter, which is more like $\frac{\alpha_s}{\pi} C_F \ln^2 y$ than $\frac{\alpha_s}{\pi}$, which appears in the expansion of σ_{tot} . But $\frac{\alpha_s}{\pi} C_F \ln^2 y \simeq 1.0$ for $y = 0.02$ and $\frac{\alpha_s}{\pi} = 0.05$.

The evaluation of the differential 3-jet cross section in $O(\alpha_s^2)$ is completely analogous to the calculation of $\sigma_{2\text{-jet}}$ in $O(\alpha_s)$. The virtual contributions (see Fig. 7) are regularized by introducing the arbitrary dimension $n = 4-2\epsilon$. Then the infrared and mass singularities appear as poles in ϵ . The same pole terms are encountered, if the real contributions (Fig. 8) are integrated over similar strips as shown in Fig. 5, except for some different boundaries, which depend now also on variables describing the 3-jet final state. Then the ϵ -pole terms cancel in the sum of virtual and real contributions and yields a finite cross section, which now depends on $\ln y$. The result is [12]

$$\frac{1}{\sigma_0} \frac{d^2\sigma}{dy_{13} dy_{23}} = \frac{\alpha_s(q^2)}{2\pi} C_F \left\{ T^V(y_{13}, y_{23}) \left[1 + \frac{\alpha_s(q^2)}{2\pi} (J_1 + J_2 + J_3) \right] + \frac{\alpha_s(q^2)}{2\pi} f(y_{13}, y_{23}) \right\} \quad (2.9)$$

where f is defined in (2.14) of [2] (it is identical to F in (2.21) of Ellis et al. [1]) and J_1, J_2 and J_3 have the simple form

$$\begin{aligned} J_1 &= C_F \left(-2 \ln^2 \frac{y}{y_{12}} - 3 \ln y - 1 + \frac{\pi^2}{3} + 2 \frac{y}{y_{12}} \ln \frac{y^2}{y_{12}} \right) \\ J_2 &= N_C \left(\ln^2 \frac{y}{y_{12}} - \ln^2 \frac{y}{y_{13}} - \ln^2 \frac{y}{y_{23}} - \frac{11}{6} \ln y + \frac{67}{18} + \frac{\pi^2}{6} - \frac{y_{12}}{3 y_{13} y_{23}} - \frac{1}{TV} \right. \\ &\quad \left. - \frac{y}{y_{12}} \ln \frac{y^2}{y_{12}} + \frac{y}{y_{13}} \ln \frac{y^2}{y_{13}} + \frac{y}{y_{23}} \ln \frac{y^2}{y_{23}} \right) \\ J_3 &= \frac{N_F}{2} \left(\frac{2}{3} \ln y - \frac{13}{9} + \left(\frac{2 y_{12}}{y_{13} y_{23}} + TS \right) \frac{1}{3TV} \right) \quad (2.10) \end{aligned}$$

T^V was defined in (2.2) and TS is the lowest order matrix element for the production of scalar gluons, which is

$$T^S(y_{13}, y_{23}) = \frac{y_{13}}{y_{23}} + \frac{y_{23}}{y_{13}} + 2 \quad (2.11)$$

We notice, that J_1 is equal to the factor of $\frac{\alpha_s}{2\pi}$ in the equation for $\sigma_{2\text{-jet}}(y)$, including the term $\sim y \ln y$, in the limit $y_{12} \rightarrow 1$. This is a necessary condition and shows that J_1 is correct. Similar tests are possible for J_2 and J_3 and have been done also in connection with the (ϵ, δ) calculation [2]. J_1, J_2 and J_3 can also be compared with a formula derived by Kunszt [1]. They differ from (2.10) by a term $\frac{\pi^2}{3}$ in J_1 ,

$\frac{\pi^2}{6}$ in J_2 , $-\frac{1}{3}$ in J_3 and some small terms proportional to y_{12} and T^S in J_2 and J_3 . We should remark, however, that Kunszt's ansatz was different, so there is no necessity for agreement. It should be kept in mind, nevertheless, that our J_1, J_2 and J_3 agree with Kunszt's formulas in the dominant terms for $y \rightarrow 0$ proportional to $\ln^2 y$ and $\ln y$.

From (2.9) one can calculate all distributions for 3-jet production one is interested in. For example, in Fig. 9 we present the thrust (T) distribution. For 3-jets thrust is equal to

$T = \max(1-y_{13}, 1-y_{23}, 1-y_{12})$. In Fig. 9 $\frac{1}{\sigma} \frac{d\sigma}{dT}$ is shown as a function of T for $y = 0.04, 0.02$ and 0.01 and $\alpha_s = 0.17$ in the \overline{MS} renormalization scheme (σ is the total cross section following from (1.2) with $N_f = 5$). We see that with y values between 0.04 and 0.02 the $O(\alpha_s^2)$ corrected distribution lies near the lowest order $O(\alpha_s)$ cross section with the same α_s value. Presumably also $y = 0.015$ would be possible. In this case the full curve will slightly lie below the $O(\alpha_s)$ curve. The curve for $y = 0.01$ deviates already appreciably from the $O(\alpha_s)$ curve so that one would conclude that this cut-off value is already outside the range of $O(\alpha_s^2)$ perturbation theory.

The way, how the 3-jet thrust distribution changes with y , shown in Fig. 9, is characteristic for QCD, i.e. a theory with non-abelian gluons. If we put $N_C = 0$, which is equivalent to a quark-gluon theory with abelian gluons, we obtain the curves in Fig. 10. We see that $\frac{1}{\sigma} \frac{d\sigma}{dT}$ decreases with decreasing y much stronger than in Fig. 9. Perhaps this is an interesting method to establish that gluons bear colour as in QCD. The term $\sim N_f$ was left unchanged. This has to be adjusted for a QED type theory.

The most direct way to compare the formulas (2.9) is via a cluster analysis in which the effects of hadronization are eliminated and the direct distribution in jet variables for 3-jets is obtained. The result of such an analysis by E. Elsen [10] of the JADE group at PETRA is shown in Fig. 11 for two values of y . The curves come from (2.9). The result for α_s is: (a) for $y = 0.04$, $\alpha_s = 0.16 \pm 0.01$, (b) $y = 0.02$, $\alpha_s = 0.173 \pm 0.015$. Of course, the α_s should be independent of y . The range of α_s values for various y is an indication of the error inherent

in this method of analysis. Unfortunately it seems difficult to go to very much smaller values of Y . In Fig. 12 we present a similar comparison with (ϵ, δ) -cuts [2]. The experimental data come from the same experiment and $\alpha_s = 0.20 \pm 0.02$. $\alpha_s = 0.20 \pm 0.02$ gives $\Lambda = (1.0 \pm 0.4)$ GeV with the second order formula. The re-normalization scheme is always the \overline{MS} scheme.

3. Sum of 3-Jet and 4-Jet Cross Section.

Although we already stated that $\frac{1}{\sigma} \frac{d\sigma}{dT}$ for 3-jet should be considered only for Y values in the range 0.01 to 0.05 one can ask how the sum of the 3-jet and 4-jet thrust distribution behaves as a function of Y . This will allow us to make the comparison with results of the other groups [1]. For this purpose we write the thrust distribution in the form

$$\frac{1}{\sigma} \frac{d\sigma}{dT} = \frac{\alpha_s}{\pi} A_0(T) + \left(\frac{\alpha_s}{\pi}\right)^2 A_1(T) \quad (3.1)$$

Instead with σ we normalized the distribution with the zero order cross section σ_0 so that $A_0(T)$ and $A_1(T)$ are independent of the value of α_s . $A_0(T)$ gets contributions from the $O(\alpha_s)$ 3-jet terms (Fig. 4), whereas $A_1(T)$ consists of the sum of the 3-jet contribution, as for example shown in Fig. 9 for 3 particular Y 's, and the 4-jet contribution. It is clear, that, as much as $A_1(T)$ from 3-jets decreases with decreasing Y , the 4-jet term in $A_1(T)$ will increase, so that the sum of both might be roughly independent of Y . Unfortunately this is not the case. We show in Fig. 13 first $A_0(T)$ and second $A_1(T)$ for $Y = 0.04$ and $Y = 2.5 \cdot 10^{-3}$. We see that $A_1(T)$ increases by a factor of 2 if Y is varied from 0.04 to $2.5 \cdot 10^{-3}$. This shows that the amount of higher order corrections $\sim \alpha_s^2$ vary if we add 3-jet and 4-jet contributions with the parameter Y which allows us to distinguish 3-jets from 4-jets. For $Y = 0.04$ the $O(\alpha_s^2)$ corrections amount to an increase of roughly 50% whereas for $Y = 2.5 \cdot 10^{-3}$ the increase is near 100%. The curve with $Y = 2.5 \cdot 10^{-3}$ agrees roughly with the predictions of the authors

in [1]. Fig. 14 shows the result taken from Kunstz's paper, which agrees with the results of all the other papers in [1]. Thus in terms of the theory presented here, the results of [1] are equivalent to $\frac{1}{\sigma} \frac{d\sigma}{dT}$ for 3 + 4-jets with a Y value near 10^{-3} . In Fig. 15 and 16 we see how $A_1(T)$ is composed of the two components 3-jet and 4-jet for $Y = 0.04, 0.01$ and 0.0025 . At the largest Y and for T below 0.8 we have roughly an equal amount of 3-jet and 4-jet, whereas for $Y = 0.01$ the 3-jet contribution is already negative (except for small T) and the 4-jet contribution is large. At $Y = 2.5 \cdot 10^{-3}$ the 4-jet is large, also the 3-jet contribution, but with a negative sign for all T . A large cancellation takes place in the sum with the result that $A_1(T)$ increased by a factor of 2 between $Y = 0.04$ and $Y = 2.5 \cdot 10^{-3}$. It is clear that it does not seem to be very economic to test the virtual higher order 3-jet diagrams (Fig. 7), which are buried in the very negative 3-jet curve of Fig. 16, which is largely influenced by 4-jet diagrams and then to add the huge 4-jet contribution. Furthermore a separation in 3-jet and 4-jet is actually senseless at $Y = 2.5 \cdot 10^{-3}$ since $\frac{d\sigma}{dT}$ (3-jet) becomes negative. If at all, only the sum of 3-jet and 4-jet might be considered there. In order to see how $A_1(T)$ behaves as a function of Y , I have studied it for Y^{-1} between 25 and 2400 in four T bins starting at $T = 0.75, 0.80, 0.85$ and 0.90 respectively with a width of $\Delta T = 0.0125$. This was necessary because the 4-jet contribution can be calculated by Monte-Carlo integration only. The results are seen in Fig. 17. For all T bins $A_1(T)$ increases with $\ln Y^{-1}$ up to the highest Y^{-1} value considered, almost linearly with $\ln Y^{-1}$. The linear increase with $\ln Y^{-1}$ has to do with the fact that the thrust variable is not unique. Thrust from a 3-parton final state is a different quantity compared to thrust calculated from a 4-parton final state. But in Fig. 17 the thrust distributions from a 3-parton cross section and a 4-parton cross section are superimposed. This was originally advocated by Schierholz [13] as an explanation for the different results obtained in [1] and [2]. It was verified later by Gottschalk [14] starting from the Ellis et al. theory [1]. Fig. 17 establishes this fact also for our theory.

The points for the largest y^{-1} values have appreciable Monte-Carlo errors since $A_1(T)$ is obtained by subtracting a large number, i.e. $A_1(T)$ for 3-jets, from a large number which is $A_1(T)$ for 4-jets. This error is of the order of 10%. Therefore it is difficult to establish the asymptotic values of $A_1(T)$ for $y \rightarrow 0$ in the considered T bins. It seems that for the smaller T 's the asymptotic value might have been reached near $y^{-1} = 2400$ whereas for a T near 0.9 $A_1(T)$ still seems to increase. To obtain the asymptotic values of $A_1(T)$ for $y \rightarrow 0$ further numerical work is necessary. Since $A_1(T)$ is expected to reach a finite limit for $y \rightarrow 0$ the increase of $A_1(T)$ with $\ln y^{-1}$ must come from subtractions of terms proportional to $y \ln y^{-1}$ and/or $y \ln^2 y^{-1}$ with rather large coefficients which should be T dependent. This means that all terms proportional to \ln^2 and $\ln y$ must have cancelled in the sum of $A_1(T)_{3jet} + A_1(T)_{4jet}$. These terms in $A_1(T)_{3jet}$ and $A_1(T)_{4jet}$ could be established analytically. For example, the contribution of terms $\sim \ln^2 y$ to $A_1(T)_{3jet}$ follows from (2.10). In the limit $T \rightarrow 1$ this term is

$$A_1(T)_{3jet} = -C_F(N_C) \frac{1}{1-T} \ln \frac{1}{1-T} \ln^2 y \quad (3.2)$$

The 4-jet contribution must be equal but with opposite sign, so that these terms cancel in the sum. The same must happen with all contributions proportional to $\ln y$.

It is of interest to see how the integrated $A_1(T)$ behaves. For this purpose we have integrated $A_1(T)$ over T up to $1-y$. For $y \rightarrow 0$ the integrated $A_1(T)$ diverges like $(-\ln^4 y)$.

This is actually the case, as shown in Fig. 18, where the integrated cross section (without the factor $(\frac{\alpha_S}{\pi})^2$) for 3-jet, 4-jet and their sum is plotted. The 4-jet increases with $\ln y^{-1}$ and is positive and 3-jet finally decreases with $\ln y^{-1}$ and the sum decreases too and goes to $(-\infty)$ for $y^{-1} \rightarrow \infty$. From the curves shown it is clear that only the values for $y^{-1} < 100$ are relevant. For $y^{-1} > 100$ they lie

outside the range where perturbation theory can be applied. The sum in Fig. 18 is compensated by the 2-jet $O(\alpha_S^2)$ contribution which has opposite sign, so that the total sum is equal to $(1.986 - 0.115 N_F)$ (see (1.1)). This has not been verified yet. The asymptotic term of the 2-jet cross section is (without the factor $(\frac{\alpha_S}{\pi})^2$)

$$\sigma_{2-jet}(y) = \frac{1}{2} C_F^2 \ln^4 y \quad (3.3)$$

whereas the asymptotic behaviour of the sum of 3-jet and 4-jet in Fig. 18 is

$$\sigma_{3-jet}(y) + \sigma_{4-jet}(y) = -\frac{1}{2} C_F^2 \ln^4 y \quad (3.4)$$

As the last point of this section we discuss the relation of the theory presented so far with the results of authors in [1]. In [1] a rather different route was taken, in order to obtain an infrared finite thrust distribution $\frac{1}{\sigma} \frac{d\sigma}{dT}$ (or $\frac{1}{\sigma} \frac{d\sigma}{dC}$ in the first and second paper of [1]). They defined as "3-jet cross section"

$$d\sigma_3 = d\sigma_1 + \int_0^{y_c} dy_{13} dv \frac{d\sigma}{2\pi} [d\sigma_4(y_3^{-1} \text{ part})] \quad (3.5)$$

where the 4-parton phase space was originally

$$d^4(\text{phase space}) \sim dy_{123} dy_{134} dy_{13} dv \frac{d\sigma}{\pi} \quad (3.6)$$

The integral in (3.6) consists of two pieces

$$d\sigma_4 = d\sigma_4(\text{singular}) + [d\sigma_4 - d\sigma_4(\text{singular})] \quad (3.7)$$

The integral with the first term in (3.7) is evaluated analytically in n -dimensional regularization and is combined with $d\sigma$ to cancel the infrared singularities ϵ^{-2} and ϵ^{-1} . It has a structure like our (2.9) but is not identical to it. The second part in (3.7) is added since in the analytical integration of the first piece not all Y_C independent terms are correctly obtained because of the approximation used for $d\sigma_4$ consisting of the singular terms only. This second part in (3.7) is computed numerically in (3.6). For $Y_{13} > Y_C$ the usual 4-jet cross section is added with identical results to ours. For Y_C some value much larger than our 0.04 may be taken then. In (3.6) the 4-parton phase space is used. Therefore the integral over the second piece in (3.7) converges at the lower limit of integration. Second, when the T - or C -distribution is calculated from $d\sigma_3$, the 3-particle T or C is used in $d\sigma_V$ and $d\sigma_4$ (singular) but not in the second term of $d\sigma_4$ in (3.7). At values of Y_{13} near 10^{-3} the approximation of $d\sigma_4$ by its singular terms $d\sigma_4$ (singular) is almost exact [15] so that the region of $0 \leq Y_{13} \leq 10^{-3}$ of the second term of (3.7) gives a negligible contribution. Therefore for the integral over $d\sigma_4 - d\sigma_4$ (singular) is cut-off at the lower limit of integration near $Y_{13} = 10^{-3}$. Thus this theory is equivalent to our formulation with an effective $Y \approx 10^{-3}$ independent where Y_C was chosen. If Y_C is equal to 10^{-3} the second part of (3.7) does not contribute at all. But the 4-parton T or C definition is then automatically used up to $Y = 10^{-3}$. In Fig. 17 we have given the results of Ellis and Ross [1] for $A_1(T)$ as horizontal lines. They cross our curves near $Y^{-1} = 1000$.

Whether there is complete agreement with our results or not must be left open in the moment. The results in [1] are taken as the asymptotic values for $Y \rightarrow 0$, whereas our values still seem to rise for $Y < 10^{-3}$. On the other hand the results of Ellis and Ross are obtained with a larger bin size, $\Delta T = 0.025$ instead of our $\Delta T = 0.0125$.

In the meantime we studied also the dependence of $A_1(T)$ on the cut-off parameters ϵ and δ . With the constraint $\epsilon = \frac{1}{2}(1 - \cos\delta)$ we found that $A_1(T)$ approaches roughly the same values as in Fig. 17

for $Y^{-1} = 2400$ if we take $\epsilon^{-1} > 100$. Thus the increase of $A_1(T)$ with decreasing parameter, which is used for the separation of 3- and 4-jets occurs independent of what definition for the separation is used. If in (3.5) Y_C would be chosen below 10^{-3} the resulting $A_1(T)$ is the same, since near $Y_C = 10^{-3}$ the asymptotic behaviour is supposed to set in. We conclude that the evaluation of the sum of 3-jet and 4-jet cross section as presented in [1] (presumably also in the case of Vermaseren at al. [1]) is equivalent to our results if the invariant mass cut-off is effectively near $Y_{\text{eff}} = 10^{-3}$.

The procedure devised originally by Ellis et al. [1] and later adopted also by the other authors in [1], is presumably a legitimate way to obtain infrared finite distributions in thrust T , C or other variables. One must admit, however, that it consists essentially of a superposition of 3- and 4-parton contributions near $Y = 0$. Then the problem is more, how to compare their results to experimental data. This seems to be difficult, because it amounts, suppose even, that quarks and gluons would be observable, to use in the analysis of the experimental data the same definitions for "3- and 4-jet cross section" as in (3.5) and (3.7). If phrased in terms of our description it means that 3-partons and 4-partons must be distinguishable down to invariant masses at least up to $(10^{-3} \cdot q^2)^{\frac{1}{2}} \approx 1$ GeV for PETRA energies.

Recently T. Gottschalk has devised algorithms which produce averaging of the genuine 4-jet contributions in (3.5) into 3-jets for all Y_{ij} below a chosen Y_{av} [14]. He was able to show that he could reproduce our original results [2] with (ϵ, δ) constraints if the averaging was done in accordance with the ϵ, δ -criteria [15]. This additional averaging seems artificial and is certainly not unique, if superimposed on the Ellis et al. theory. It has to be done from the beginning in connection with the cancellation of infrared singularities, as we did it.

Of course, things get more complicated if we are more realistic and take into account that quarks and gluons are not directly observable and are detected only through their hadronic debris. Then the question arises whether the theory with large $Y \approx 0.05$ or a very

small $y \lesssim 10^{-3}$ should be used to describe the primordial production of quarks and gluons in a perturbative framework. The more or less unanimous opinion is, that it would not make sense to use invariant mass values to separate 3- and 4-jet contributions much below the nonperturbative jet spread caused by the decay of quarks and gluons into hadrons. At PETRA energies this nonperturbative spread is of the order of 0.05 to 0.1 if measured in m^2/q^2 (see Fig. 19) [18]. This means, that y values very much below 0.05 should not be used in Monte-Carlo programs, in which the hadronization is described by a procedure developed in connection with $O(\alpha_s)$ perturbative calculations [16].

4. Summary and Concluding Remarks.

In this report we have described the results of a new calculation of $O(\alpha_s^2)$ corrections for jet distributions on the basis of an invariant mass constraint for separating 3- and 4-jet contributions. In this framework we have compared our results to that of Ellis et al. [1]. This theory is essentially equivalent to using $y \approx 10^{-3}$ for the 3-, 4-jet separation or even smaller values down to $y \rightarrow 0$. First, in this range of y values experimental data based on cluster analysis, in which the hadronization is unfolded, cannot be compared with theory. Second, any refinements, in which the hadronization of quarks and gluons is added on the basis of models already available the y should be of the order of the nonperturbative jet spread [17], which is y near 0.05. Certainly varying y in reasonable limits should be tried and it is to be seen whether final statements about α_s depend on y or not.

Concerning the discrepancy between the results of Ellis et al. [1] and ours [2] we found that both results agree in the limit where the two different definitions of "thrust" are identical. Gottschalk [14] had demonstrated this earlier by starting from the Ellis et al. theory and introducing our definition of "thrust", which means using large mass cut-offs y . In this work we have shown it by starting from our theory [2] and evaluating it at very small y values and this way approaching the "thrust" definition of Ellis et al. [1].

Acknowledgements: I thank G. Schierholz, F. Gutbrod and A. Ali and many other colleagues for numerous discussions and E. Eisen for supplying me with his results of the cluster analysis of the JADE data before publication. Furthermore I would like to thank G. and J. Ranft for their kind hospitality at the meeting in Bad Schandau.

References:

- [1] R.K. Ellis, D.A. Ross, A.E. Terrano, Phys. Lett. 45, 1226 (1980) and Nucl. Phys. B 178, 421 (1981)
Z. Kunszt, Phys. Lett. 99 B, 429 (1981), 107 B, 123 (1981)
J.A.M. Vermaseren, K.F.J. Gaemers, S.J. Oldham, Nucl. Phys. B 187, 301 (1981)
L. Clavelli, D. Wyler, Phys. Lett. 103 B, 383 (1981)
R.K. Ellis, D.A. Ross, Phys. Lett. 106 B, 88 (1981)
A. Ali, DESY-report 81-051, September (1981)
T. Gottschalk, Phys. Lett. 109 B, 331 (1982)
- [2] K. Fabricius, I. Schmitt, G. Schierholz, G. Kramer, Phys. Lett. 97 B, 431 (1981); Z. Physik C 11, 315 (1982)
See also S. Sharpe, Phys. Lett. 106 B, 331 (1981)
- [3] W. Celmaster, R.J. Gonsalves, Phys. Rev. D 20, 1420 (1979)
- [4] K.G. Chetyrkin, A.L. Kataev, F.V. Tkachov, Phys. Lett. 85 B, 277 (1979)
M. Dine, J. Sapirostein, Phys. Rev. Lett. 43, 668 (1979)
W. Celmaster, R.J. Gonsalves, Phys. Rev. Lett. 44, 560 (1979); Phys. Rev. D 21, 3112 (1980)
- [5] TASSO Collaboration, R. Brandelik et al., DESY report 82-101 (February 1982)
- [6] A. Ali et al., Phys. Lett. 82 B, 285 (1979); Nucl. Phys. B 167 454 (1980)
- [7] J. Dorfan, Z. Physik C 7, 349 (1981)
H.J. Daum, H. Meyer, J. Bürger, Z. Physik C 8, 167 (1981)
K. Lanius, H.E. Roloff, H. Schiller, Z. Physik C 8, 251 (1981)
- [8] W. Braunschweig, 1981 Int. Symposium on Lepton and Photon Interactions at High Energies, Bonn
- [9] See A.J. Buras, 1981 Int. Symposium on Lepton and Photon Interactions at High Energies, Bonn and Fermilab Report 81/69
- [10] E. Elsen, private communication. These curves are still preliminary.
- [11] G. Sterman, S. Weinberg, Phys. Rev. Lett. 39, 1436 (1977)
- [12] G. Kramer, G. Schierholz, in preparation. In the final version we will include also terms $\sim \ln y$.
- [13] G. Schierholz, DESY-report 81-042 (1981)
- [14] T. Gottschalk, Phys. Lett. 109 B 331 (1982)
- [15] This was verified by T. Gottschalk as stated in a letter to A. Ali. I thank A. Ali for making the content of this letter available to me.
- [16] For example in A. Ali, E. Pietarinen, G. Kramer, J. Willrodt, Phys. Lett. 93 B, 155 (1980)
- [17] See also the statements made in G. Fox, California Institute of Technology preprint, CALT-68-863
- [18] R. Marshall, 1981 European Physical Society International Conference on High Energy Physics, Lisbon

Figure Captions:

- Fig. 1: Three-jet phase volume with (ϵ, δ) cuts.
- Fig. 2: Three-jet cross section for $(\epsilon, \delta) = (0.2, 45^\circ)$ and $(\epsilon, \delta) = (0.1, 30^\circ)$ together with the Born cross section as a function of $x_{\max} \equiv T$ for $\alpha_s = 0.17$.
- Fig. 3: The QCD prediction for the reconstructed thrust T to leading order $O(\alpha_s)$ and the QCD predictions of "two models" which include the second order $O(\alpha_s^2)$ effects.
- Fig. 4: Diagrams with two and three partons in the final state to order α_s .
- Fig. 5: Three-parton phase space in terms of Y_{13} and Y_{23} with boundary for two-jet region.
- Fig. 6: Two-jet and three-jet cross section as a function of y in units of α_s without the factor $\frac{\alpha_s}{\pi}$.
- Fig. 7: Diagrams with three partons in the final state to order α_s^2 interfering with diagrams in Fig. 4.
- Fig. 8: Diagrams with four partons in the final state.
- Fig. 9: Three-jet cross section for $y = 0.04, 0.02$ and 0.01 together with Born cross section as a function of thrust T for $\alpha_s = 0.17$.
- Fig. 10: Same as Fig. 9 for abelian gluons ($N_C = 0$) for coupling constant $\alpha_s = 0.23$ together with Born cross section equal to that in Fig. 9.
- Fig. 11: Results of a cluster analysis by E. Elsen of the JADE group [10] for (a) $y = 0.04$ and (b) $y = 0.02$ compared to (2.9). The resulting α_s is (a): $\alpha_s = 0.16 \pm 0.01$ and (b): $\alpha_s = 0.173 \pm 0.015$ and the corresponding Λ is: (a) $\Lambda = (0.40 \pm 0.15)$ GeV and (b) $\Lambda = (0.6 \pm 0.2)$ GeV.

- Fig. 12: The same as Fig. 11 with (ϵ, δ) cuts: $\epsilon = 0.2$, $\delta = 45^\circ$. The resulting α_s is $\alpha_s = 0.20 \pm 0.02$.
- Fig. 13: $A_1(T)$ as a function of thrust T for two different $y = 0.04$ and $y = 0.0025$. $A_0(T)$ is the $O(\alpha_s)$ contribution. $A_1(T)$ is the sum of 3-jet and 4-jet contributions.
- Fig. 14: $A_1(T)$ as obtained by Kunszt (his second paper in [1]).
- Fig. 15: 3- and 4-jet components of $A_1(T)$ for $y = 0.04$ and $y = 0.01$.
- Fig. 16: 3-jet and 4-jet components of $A_1(T)$ and $A_1(T)$ for $y = 0.0025$.
- Fig. 17: $A_1(T)$ for different T bins as a function of y . $A_1(T)$ is the sum of 3-jet and 4-jet contribution. The lines are drawn to direct the eye.
- Fig. 18: Integrated cross section for 3-jets and 4-jets as a function of y without factor $(\frac{\alpha_s}{\pi})^2$.
- Fig. 19: Distribution of normalized jet mass Y for $q\bar{q}$ with fragmentation from Monte-Carlo model with Field-Feynman fragmentation for $E_{\text{cm}} = 30$ GeV. The $q\bar{q} + q\bar{q}g$ curve in this model is also shown.

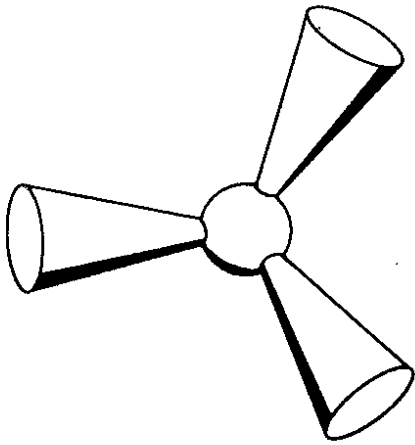


Fig. 1

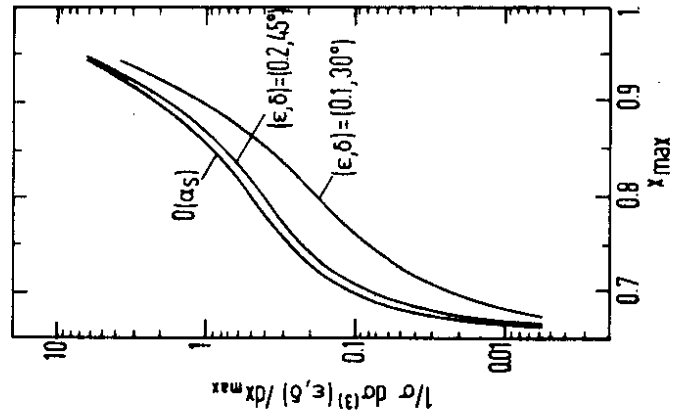


Fig. 2

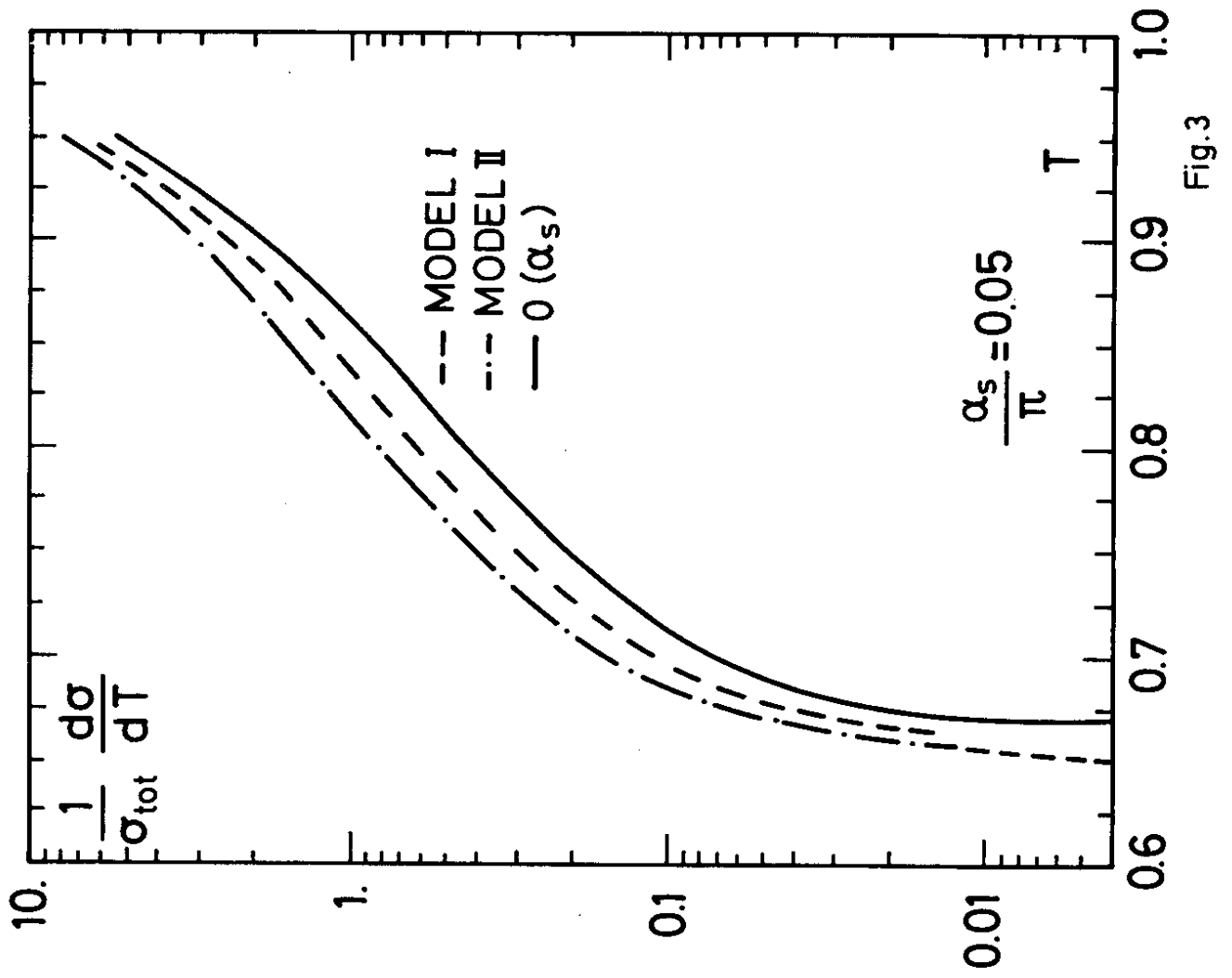


Fig. 3

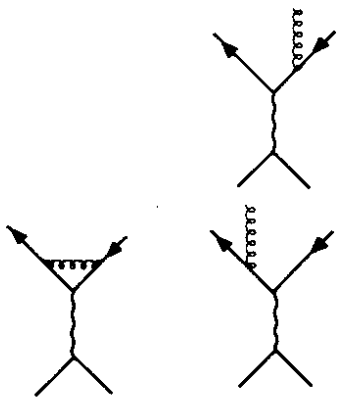


Fig.4

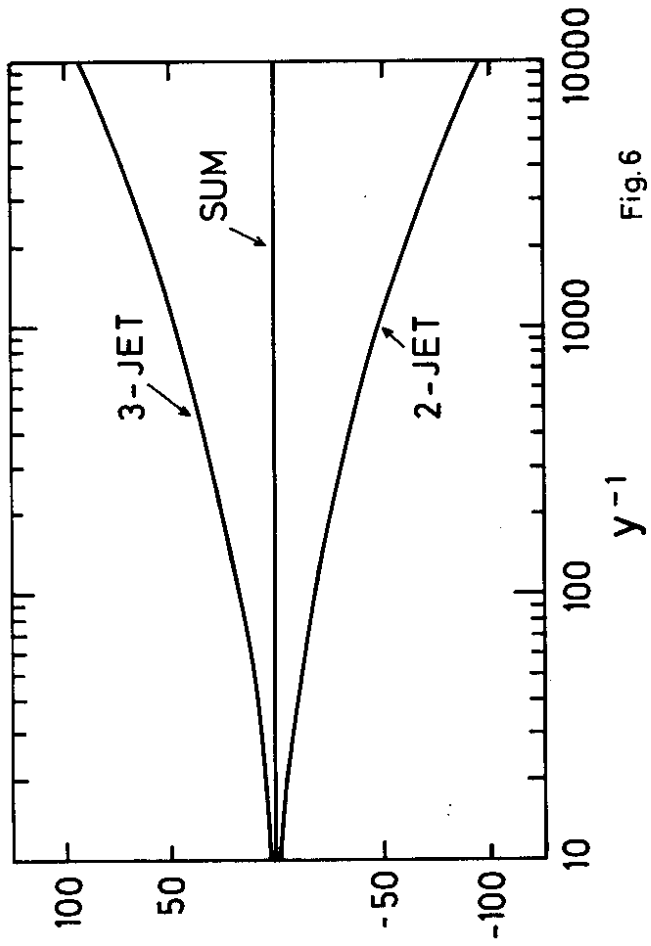


Fig.6

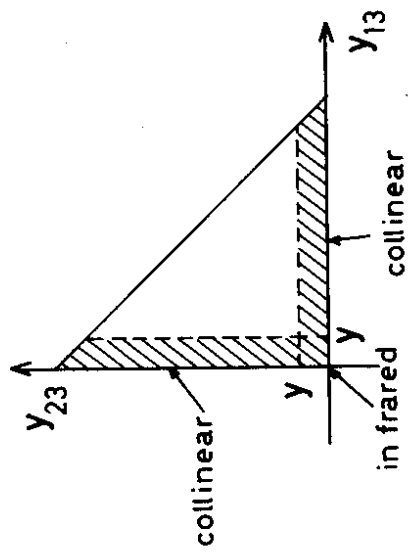


Fig.5

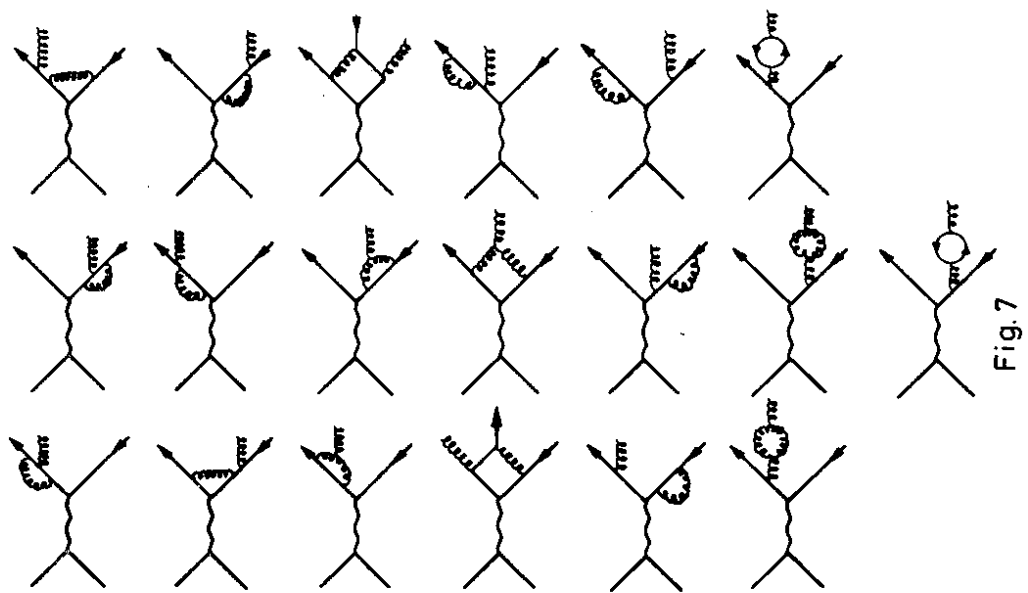


Fig. 7

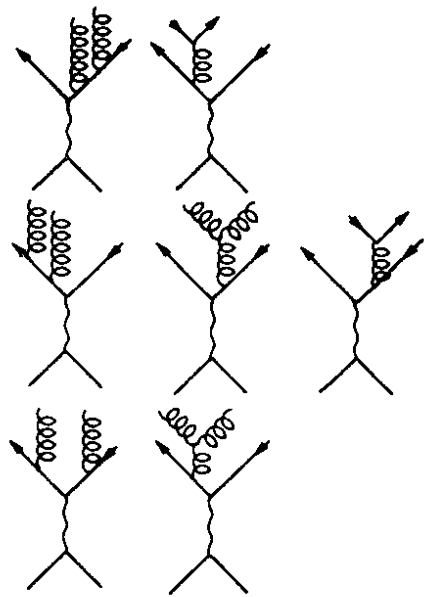


Fig. 8

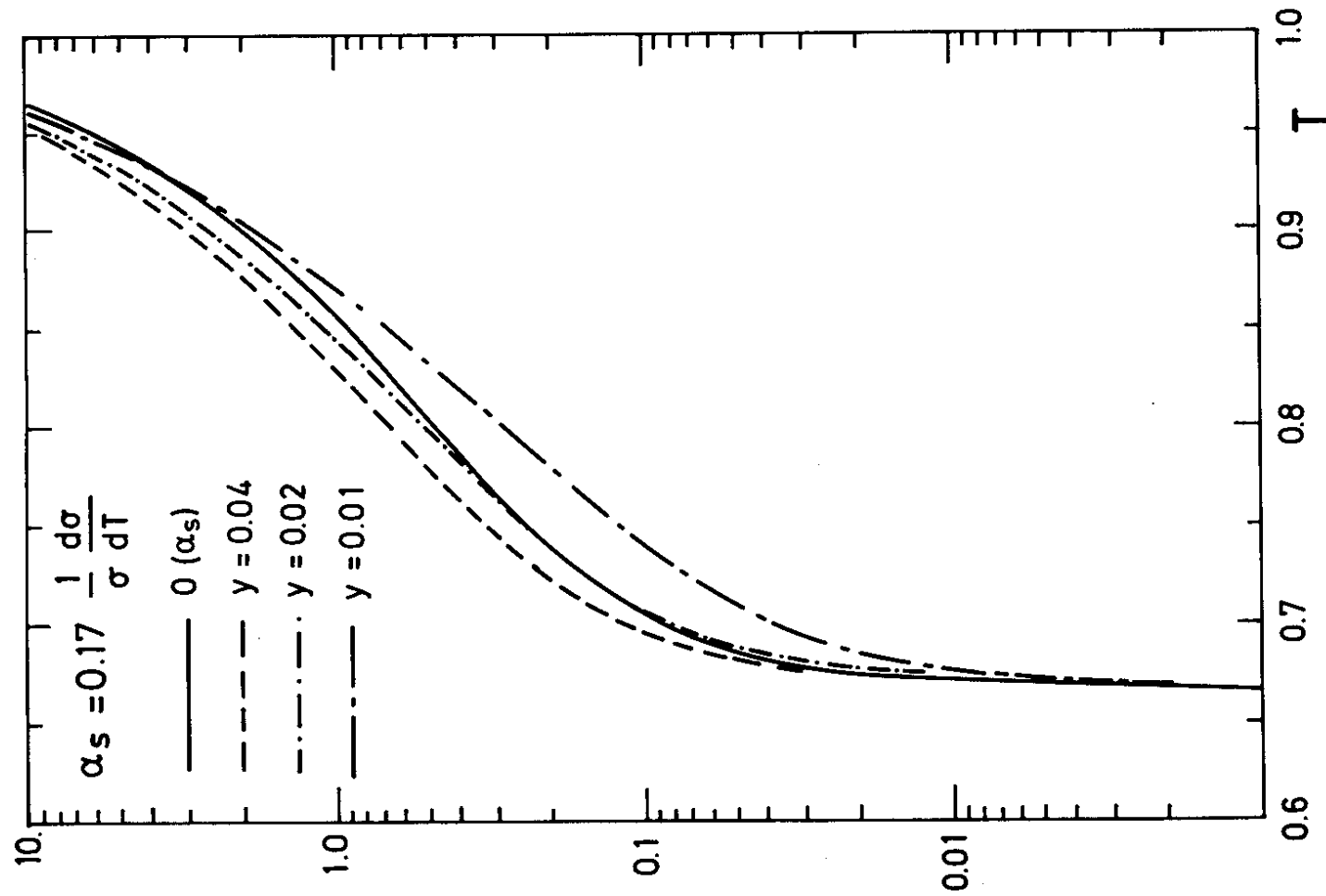


Fig. 9

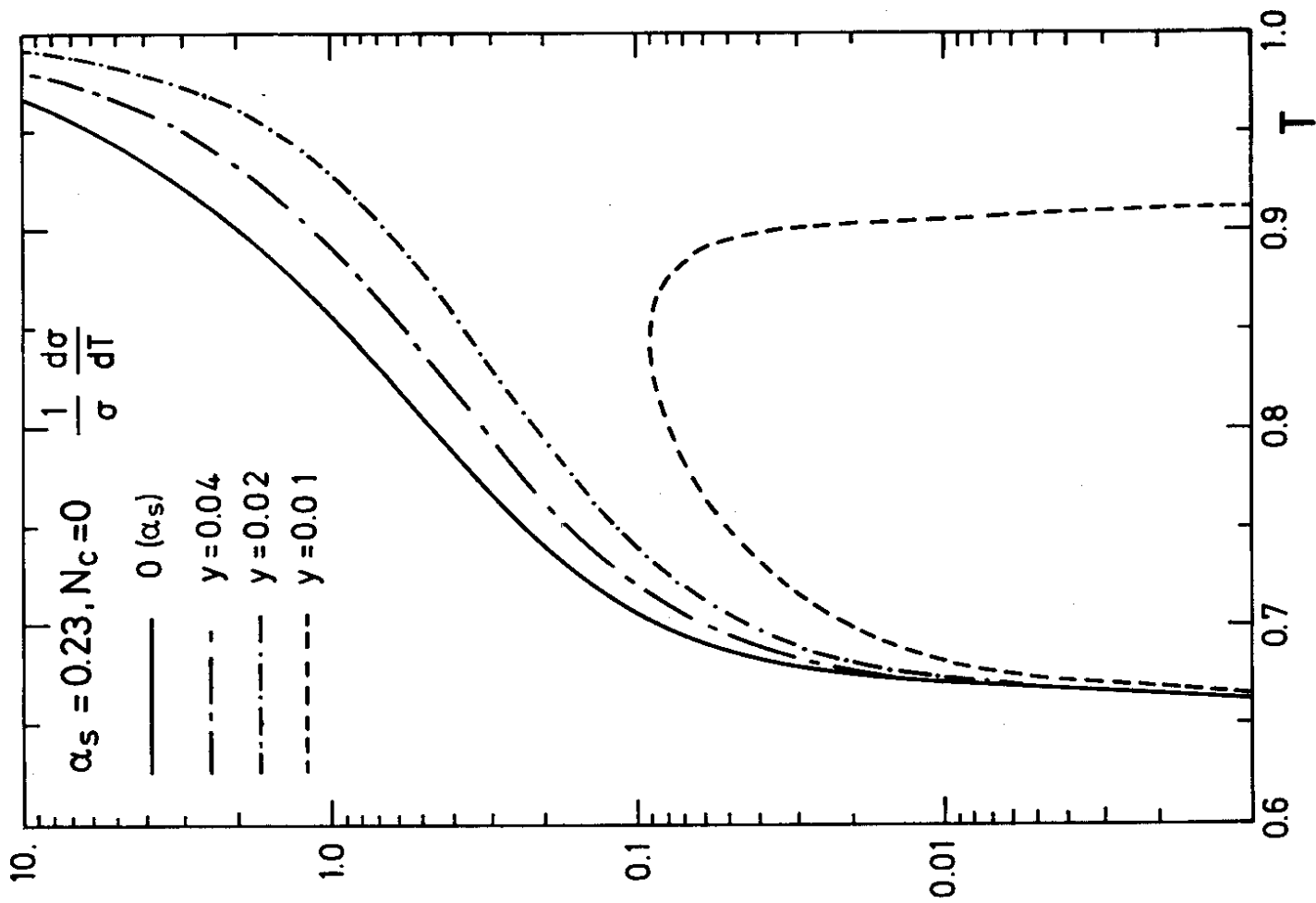


Fig. 10

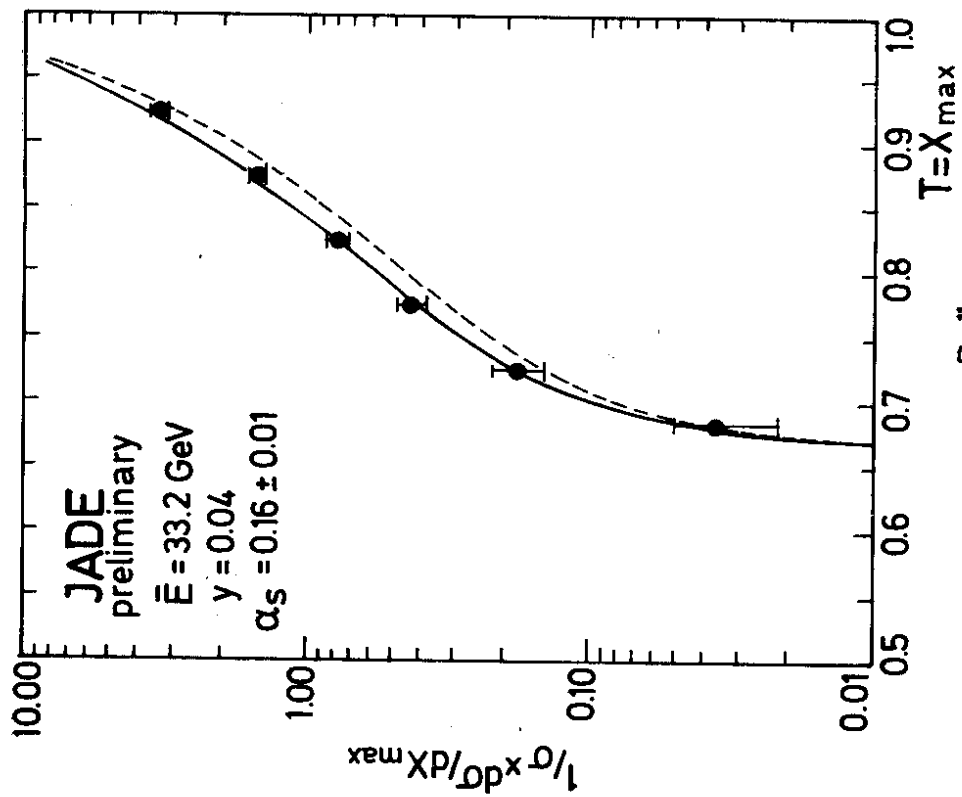


Fig. 11a

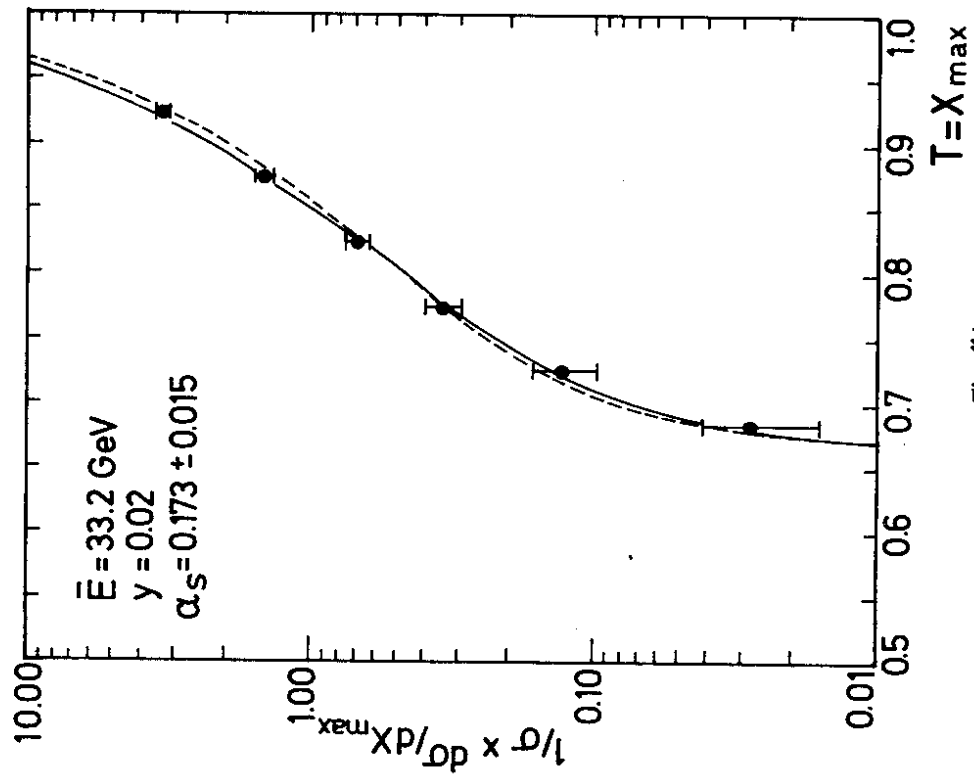


Fig. 11b

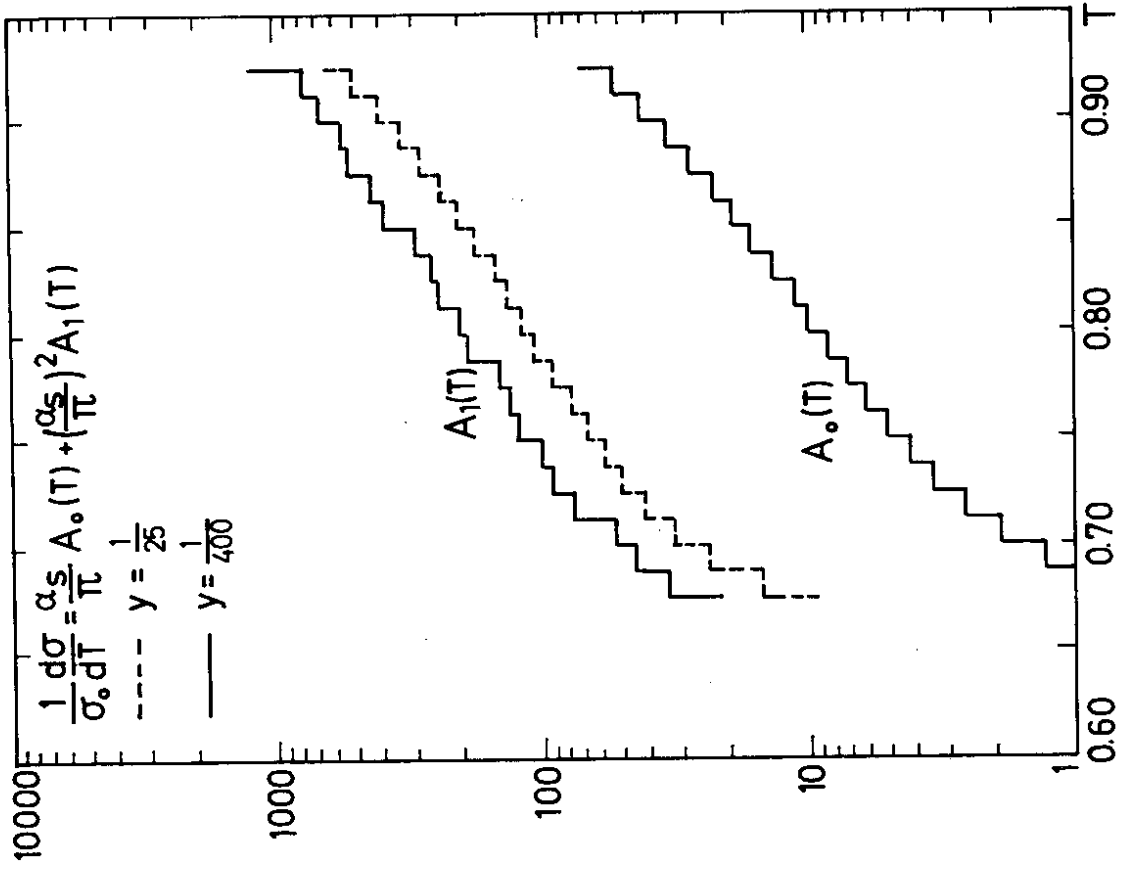


Fig.13

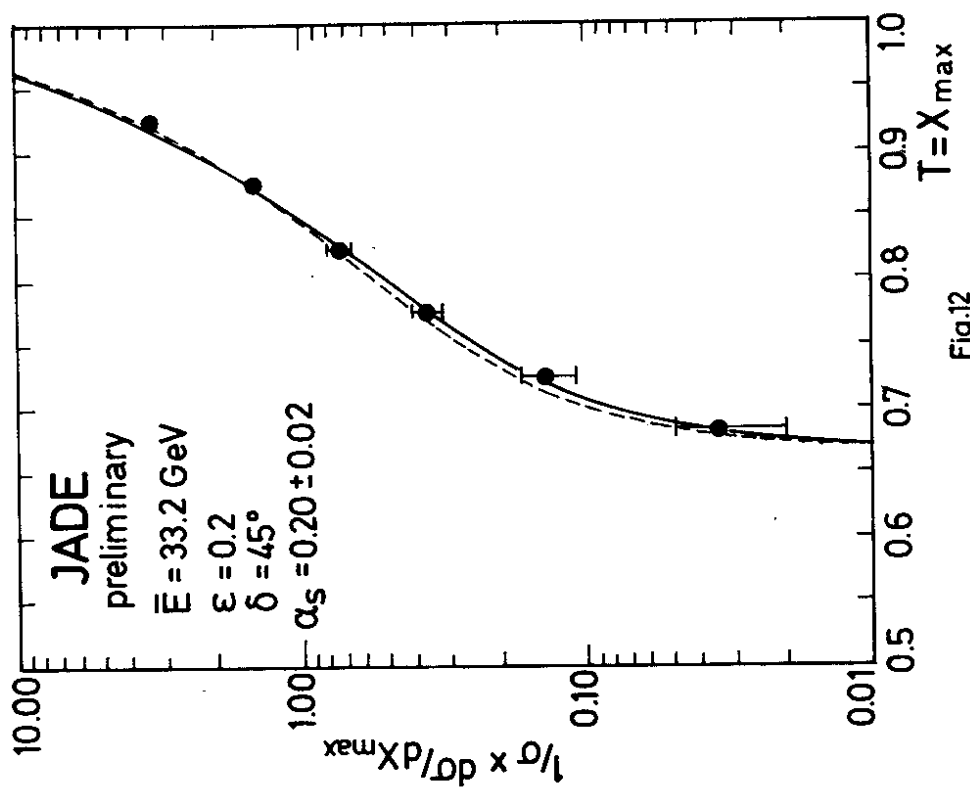


Fig.12

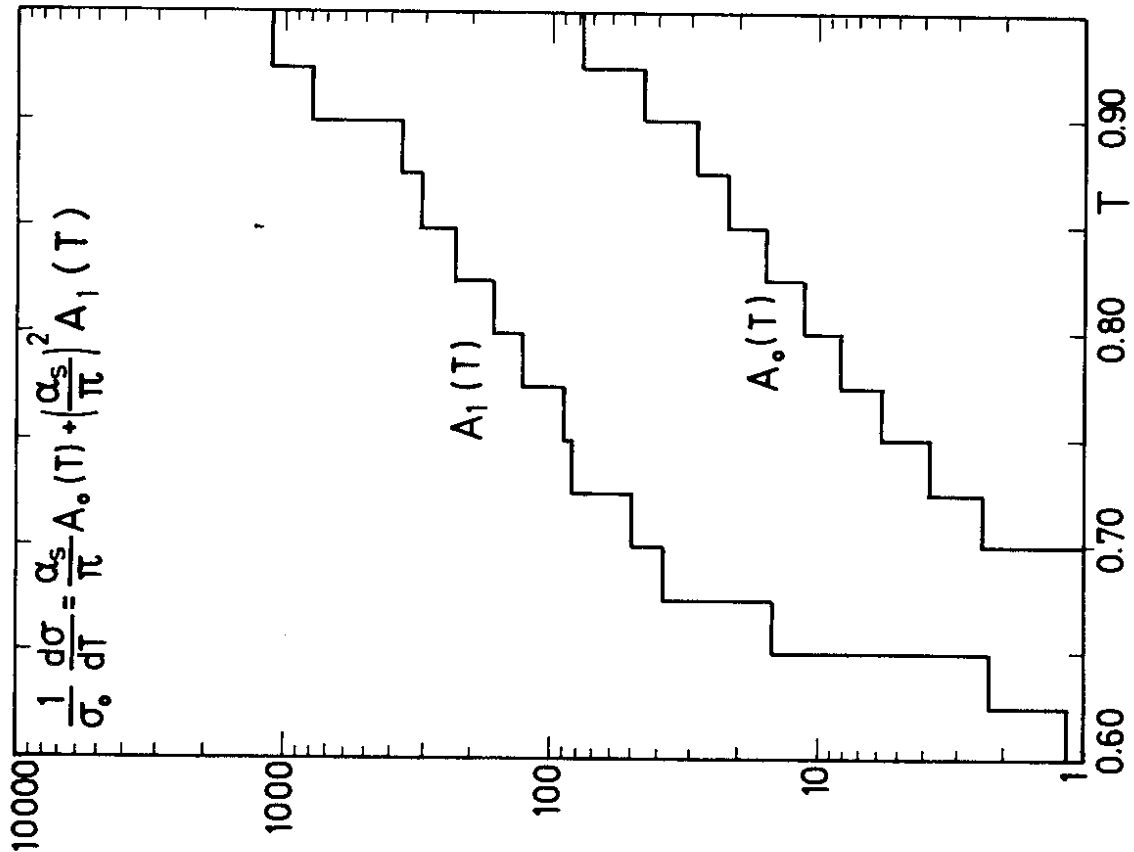


Fig. 14

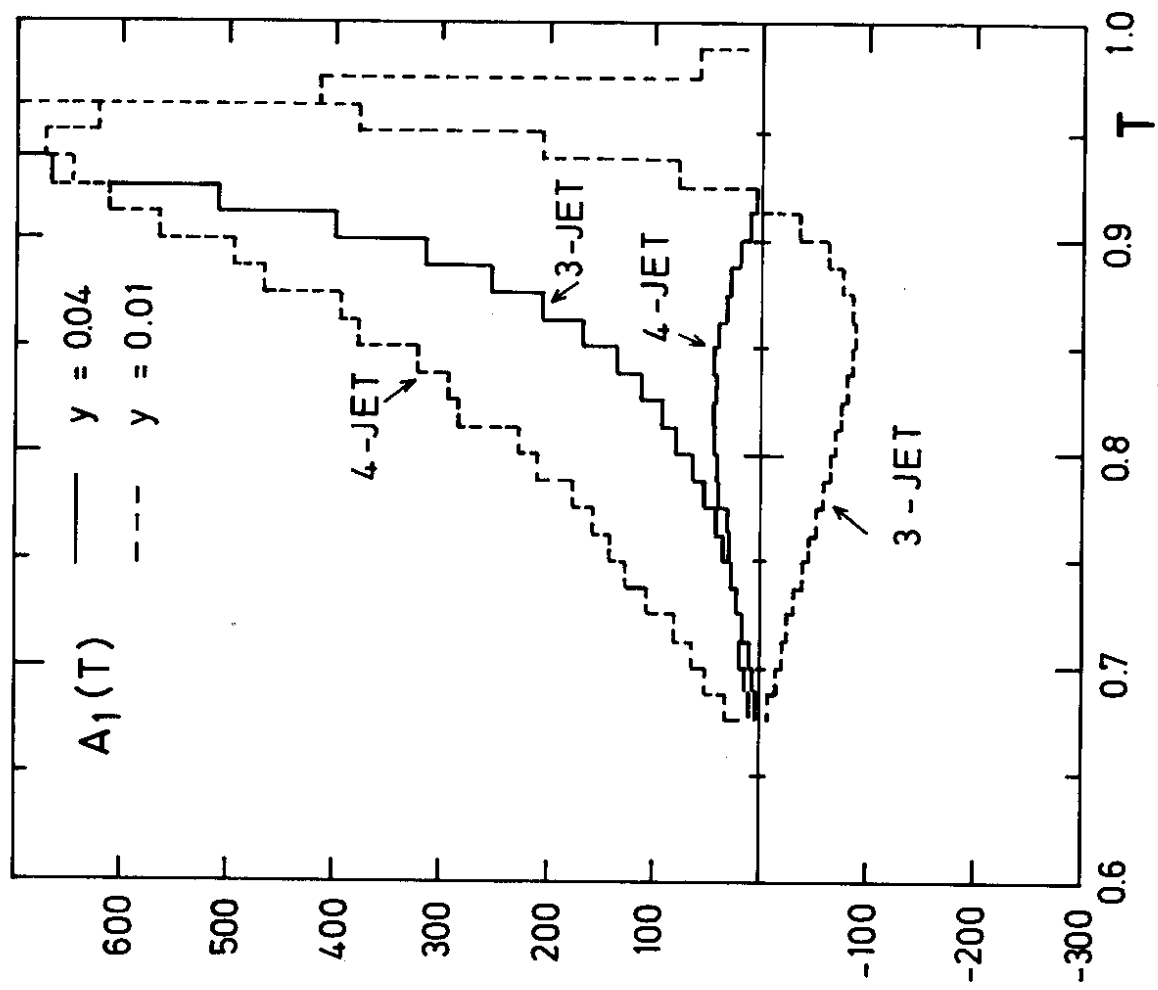


Fig. 15

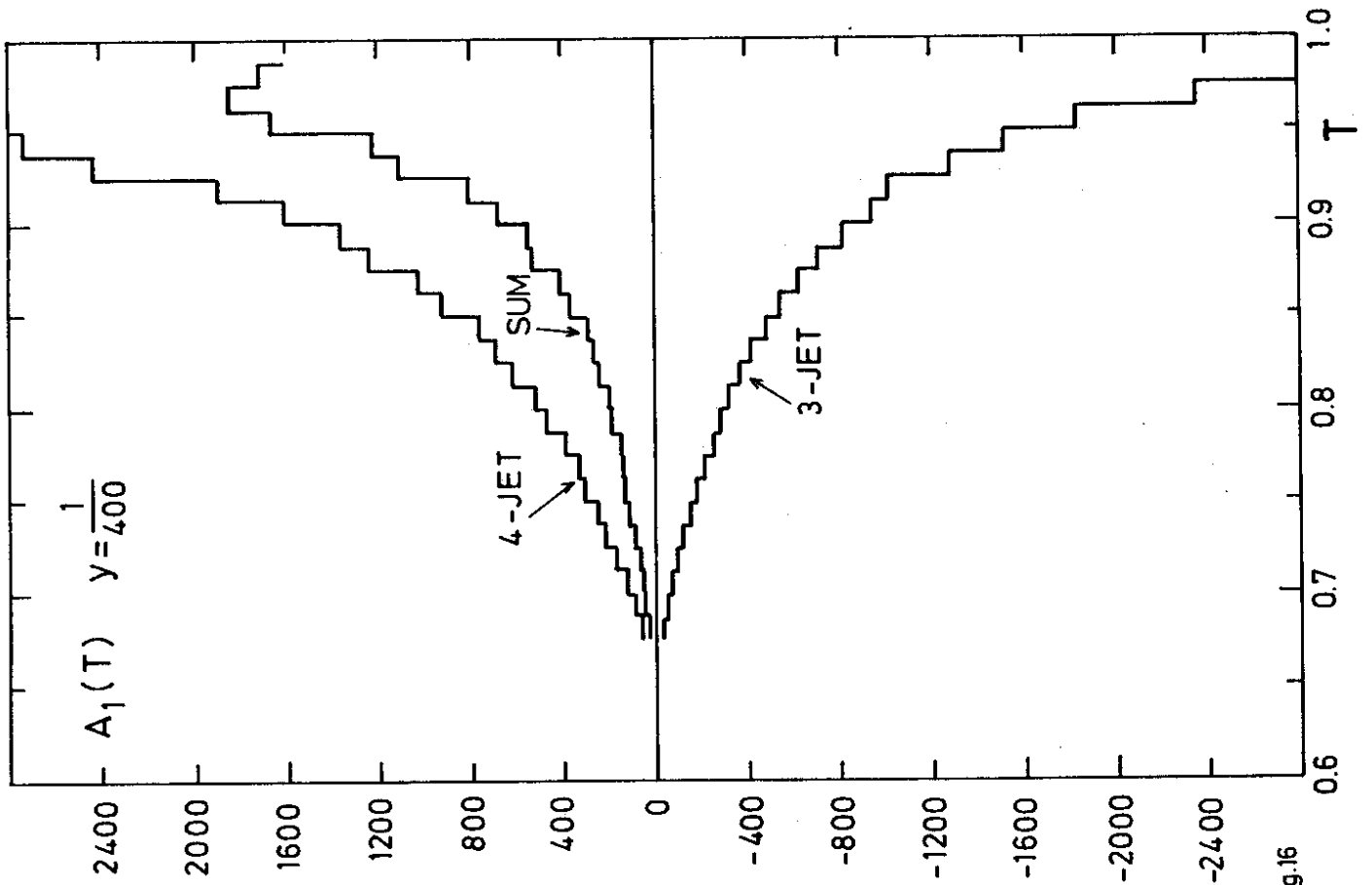


Fig.16

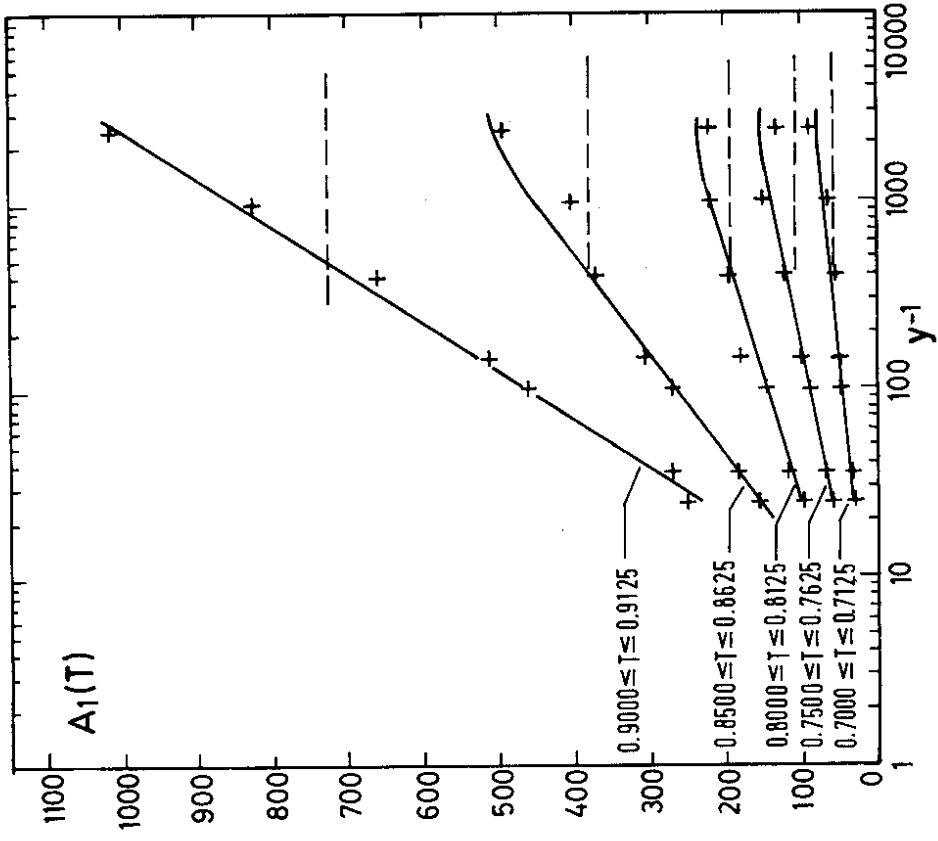


Fig.17

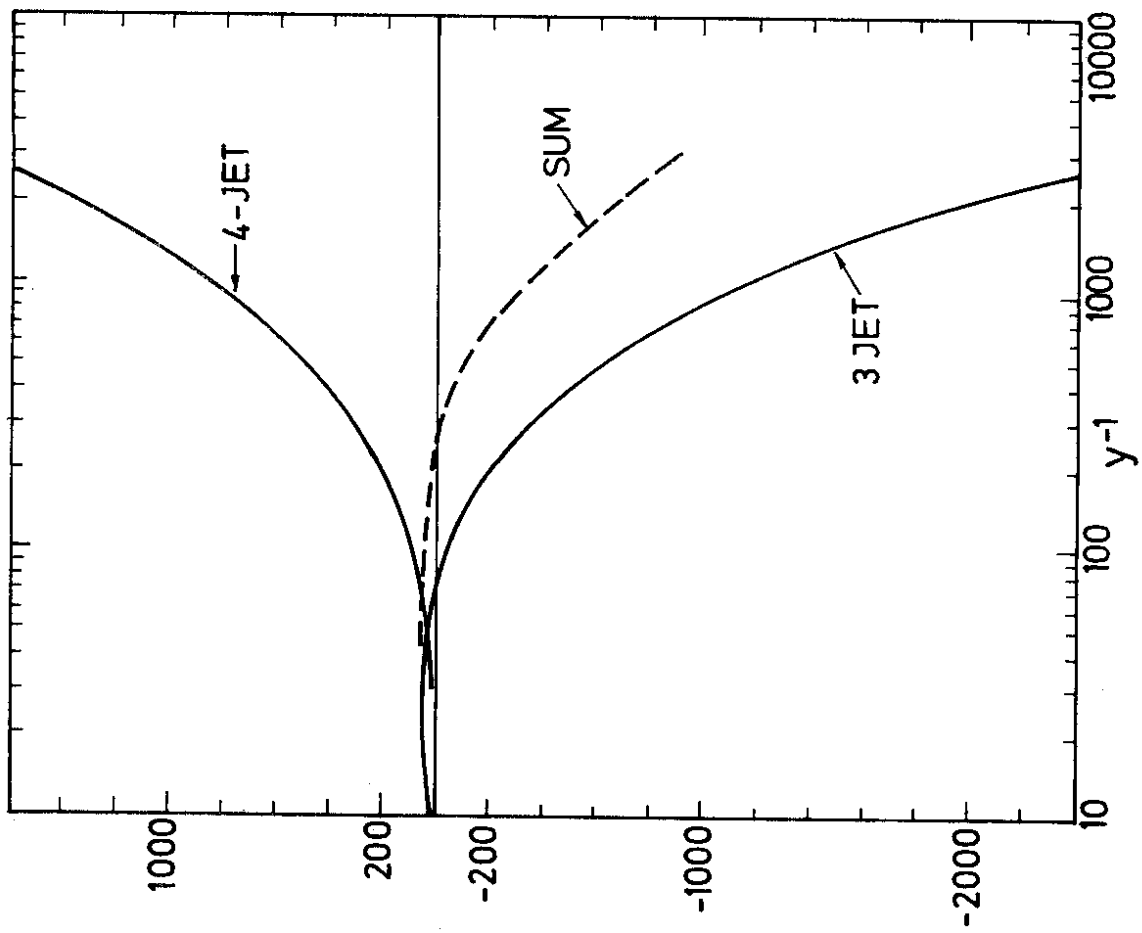


Fig.18

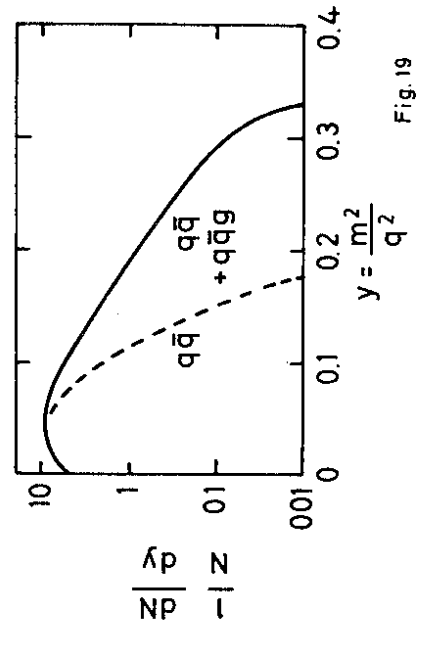


Fig.19